The sentrin-conjugating enzyme mUbc9 interacts with GLUT4 and GLUT1 glucose transporters and regulates transporter levels in skeletal muscle cells

Francesco Giorgino*†, Ottilia de Robertis*, Luigi Laviola*‡, Carmela Montrone*, Sebastio Perrini*, Karen C. McCowen‡, and Robert J. Smith‡

*Istituto di Clinica Medica, Endocrinologia e Malattie Metaboliche, University of Bari School of Medicine, I-70124 Bari, Italy; and ‡Metabolism Section, Joslin Diabetes Center, Harvard Medical School, Boston, MA 02215

Communicated by C. Ronald Kahn, Harvard Medical School, Boston, MA, December 2, 1999 (received for review September 29, 1999)

Glucose transport in insulin-regulated tissues is mediated by the GLUT4 and GLUT1 transporters. Using the yeast two-hybrid system, we have cloned the sentrin-conjugating enzyme mUbc9 as a protein that interacts with the GLUT4 COOH-terminal intracellular domain. The mUbc9 enzyme was found to bind directly to GLUT4 and GLUT1 through an 11-aa sequence common to the two transporters and to modify both transporters covalently by conjugation with the mUbc9 substrate, sentrin. Overexpression of mUbc9 in L6 skeletal muscle cells decreased GLUT1 transporter abundance 65%, resulting in decreased basal glucose transport. By contrast, mUbc9 overexpression increased GLUT4 abundance 8-fold, leading to enhanced transport stimulation by insulin. A dominant-negative mUbc9 mutant lacking catalytic activity had effects opposite to those of wild-type mUbc9. The regulation of GLUT4 and GLUT1 was specific, as evidenced by an absence of mUbc9 interaction with or regulation of the GLUT3 transporter isoform in L6 skeletal muscle cells. The mUbc9 sentrin-conjugating enzyme represents a novel regulator of GLUT1 and GLUT4 protein levels with potential importance as a determinant of basal and insulin-stimulated glucose uptake in normal and pathophysiological states.

Facilitative glucose transporters (GLUTs) are a family of structurally related, membrane-spanning glycoproteins that catalyze the transport of glucose across the lipid bilayer of the plasma membrane along a concentration gradient (1, 2). Insulin-sensitive tissues, such as skeletal muscle, myocardium, and fat, express the GLUT4 and GLUT1 transporter isoforms. In these tissues, GLUT1 is largely responsible for basal glucose transport, because a significant amount of this transporter isoform (≈40%) is present at the cell surface in the absence of insulin (3). By contrast, the majority of GLUT4 localizes to intracellular tubulovesicular structures clustered in the cytoplasm, often in close proximity with the plasma membrane (3–5). The rapid and marked augmentation of cellular glucose uptake in response to insulin is achieved through the mobilization of GLUT4 from its storage compartment, resulting in substantial increases in both cell-surface GLUT4 levels and glucose transport rates.

Targeting information contained within the primary sequences of GLUT4 and GLUT1 dictates the differential localization of the two transporter isoforms to specific cellular sites (6, 7). An NH_2-terminal Phe-Gln-Gln-Ile sequence (8) and a COOH-terminal domain including Leu^{489} and Leu^{490} (9, 10) have been suggested to mediate GLUT4 internalization, probably at the level of transporter entry into cell-surface, clathrin-coated pits or further down in the endocytic pathway (8, 11). GLUT4 targeting to the highly insulin-responsive storage compartment appears to require additional, independent signals that may be contained within the COOH-terminal 30 aa of the transporter (11, 12). The presence of specific intracellular localization signals in the NH_2 terminus and the COOH terminus of GLUT4 raises the possibility that these sequences interact with one or more cellular proteins and that this provides a mechanism for regulation of transporter trafficking and function. Proteins that associate with the GLUT4 COOH-terminal domain recently have been identified (13, 14).

Sentrin, a small ubiquitin-like protein also known as SUMO-1, PIC1, GMP1, and UBL1 (15–18), recently has been shown to be covalently linked to Ran GTPase-activating protein 1 (RanGAP1) (17–19) and other proteins (15, 16). In contrast to the well known function of ubiquitin conjugation in proteasome-mediated protein degradation, modification of RanGAP1 by sentrin does not lead to proteolysis but, rather, appears to modulate the subcellular localization of RanGAP1 (17–19). Multiple or single sentrin residues are conjugated by a pathway that is distinct from, but analogous to, ubiquitin conjugation. mUbc9, a structural homologue of the E2 ubiquitin-conjugating enzymes, is the only known enzyme capable of linking sentrin to other proteins (20) and does not catalyze ubiquitin conjugation (21). We report here that both GLUT4 and GLUT1 transporters bind directly to mUbc9 via a common COOH-terminal 11-aa sequence. We demonstrate that GLUT4 and GLUT1 are conjugated with the mUbc9 substrate, sentrin, and that mUbc9 regulates the cellular levels of the two glucose transporters in opposite directions through a posttranscriptional mechanism.

Materials and Methods

Yeast Two-Hybrid Cloning. As a bait for screening with the two-hybrid system, the vector pLexA-GLUT4 COOH-t expressing a fusion protein composed of amino acids 467–509 of rat GLUT4 linked to the DNA-binding domain of the yeast LexA transcriptional activator was constructed by PCR amplification of rat GLUT4 cDNA (provided by G. I. Bell, University of Chicago, Chicago) and subsequent subcloning into the yeast vector pBTM116 (22). The L40 yeast strain of *Saccharomyces cerevisiae* was transformed with pLexA-GLUT4 COOH-t by the lithium acetate protocol (23). Yeast expressing the pLexA-GLUT4 COOH-t fusion then were transformed with a library expressing cDNAs derived from mouse TA1 adipocytes as fusions to the VP16 activation domain (provided by S. M. Hollenberg, Oregon Health Sciences University, Portland, OR). The TA1 library was constructed by using cultures with a greater than 70% adipocyte population, contains fragments of 0.35–0.7 kb, and includes approximately 5×10^6 transformants (22). A total of 27×10^6 transformants were screened; approximately 200 colonies showed activation of the yeast reporter genes, and 80 colonies were selected that showed dependence on the LexA-GLUT4 COOH-t fusion protein for activation of reporter genes by using

Abbreviations: GLUT, glucose transporter; GST, glutathione *S*-transferase; DHFR, dihydrofolate reductase; PM, plasma membrane(s); IM, intracellular membrane(s).

†To whom reprint requests should be addressed at: Istituto di Clinica Medica, Endocrinologia e Malattie Metaboliche, University of Bari School of Medicine, Piazza Giulio Cesare, 11, I-70124 Bari, Italy. E-mail: giorginf@tin.it.

The publication costs of this article were defrayed in part by page charge payment. This article must therefore be hereby marked "*advertisement*" in accordance with 18 U.S.C. §1734 solely to indicate this fact.

a LexA-lamin fusion as a negative control. Plasmids from library clones subsequently were isolated from the yeast, transferred to *Escherichia coli*, and sequenced, and the GenBank/European Molecular Biology Laboratory databases were screened for similar sequences by using the GCG program FASTA.

Cell Lines and Transfection Studies. 3T3-L1 fibroblasts (American Type Culture Collection) were grown and differentiated into adipocytes as described (5). L6 rat skeletal muscle cells were cultured in Eagle's minimum essential medium supplemented with 10% donor calf bovine serum and nonessential amino acids in a 5% CO_2 atmosphere at 37°C. Total lysates and subcellular fractions from 3T3-L1 adipocytes or L6 myoblasts were prepared as described (24–26).

For overexpression of mUbc9 in L6 cells, the full-length mUbc9 sequence was cloned into the mammalian expression vector pcDNA3.1 (Invitrogen). A negative mutant form of mUbc9 containing Ala instead of Cys^{93} was generated by PCR-based site-directed mutagenesis by using the QuickChange site-directed mutagenesis kit (Stratagene). L6 cells were transfected at 85% confluence by using Lipofectamine (Life Technologies, Gaithersburg, MD). L6 myoblasts stably overexpressing GLUT4 were generated similarly by transfection with pCR3.1 containing the full-length rat GLUT4 cDNA sequence.

Quantitative PCR Analyses. GLUT4 and GLUT1 mRNA levels were determined by quantitative reverse transcription–PCR of total cell RNA by using the forward primer 5′-AGA GTG CCT GAA ACC AGA GG-3′ and the reverse primer 5′-CAG TCA GTC ATT CTC ATC TGG C-3′ for amplification of GLUT4 mRNA and the forward primer 5′-GAG TGC CTG AAA CCA GAG G-3′ and the reverse primer 5′-CTC ACA CTT GGG AGT CA-3′ for amplification of GLUT1 mRNA. Amplification products were electrophoresed on 1% agarose gels and stained with ethidium bromide.

Bacterial Expression of Glutathione *S*-transferase (GST) and Dihydrofolate Reductase (DHFR) Fusion Proteins and *in Vitro* Association Studies. To generate a GST fusion protein containing mUbc9 (GST-mUbc9), the full-length mUbc9 coding sequence was cloned into the pGEX-3X plasmid (Amersham Pharmacia), expressed in the *E. coli* strain DH5α, and purified according to the manufacturer's instructions. To generate hexahistidine-tagged DHFR (6xHis-DHFR) fusion proteins containing glucose transporter fragments, the GLUT4 COOH-terminal fragment (residues 467–509), the GLUT1 COOH-terminal fragment (residues 451–492), and a shorter fragment of the GLUT4 COOH-terminal region (residues 478–509) were generated by PCR amplification and cloned into pQE-40 (Qiagen). Plasmid constructs were expressed in the *E. coli* strain M15[pREP4] and purified according to the manufacturer's instructions.

To study the association between GST-mUbc9 and transporters from L6 myoblasts overexpressing GLUT4, GST-mUbc9 first was immobilized onto glutathione-Sepharose 4B beads (Amersham Pharmacia) for 1 h at 4°C in 500 μl of TNE buffer (120 mM NaCl/1 mM EDTA/1 mM PMSF/5 μg/ml leupeptin/10 mM Tris·HCl, pH 7.6); the beads (50 μl) were washed twice with 1 ml of TNE buffer at 4°C and resuspended in 150 μl of ice-cold TNE buffer. The immobilized fusion proteins were incubated for 16 h at 4°C with 150 μl of solubilized membranes (solubilization buffer: 1% Triton X-100/0.5% sodium deoxycholate/1% SDS/0.5% BSA; protein concentration, $\approx$0.5 mg/ml). The beads then were washed four times with 1 ml of TNE buffer at 4°C, and the fusion proteins were eluted by incubation with 80 μl of glutathione elution buffer (10 mM reduced glutathione/50 mM Tris·HCl, pH 8.0) for 30 min at 20°C. Eluates were resolved by SDS/PAGE and subjected to immunoblotting with anti-GLUT4, anti-GLUT1, or anti-GLUT3 antibodies.

The association between GST-mUbc9 and recombinant glucose transporter fragments fused to the 6xHis-DHFR was studied *in vitro* according to previously reported protocols (27).

Immunoprecipitation and Immunoblotting. For immunoprecipitation of glucose transporters, membranes were solubilized in PBS containing 1% Triton X-100, 0.5% sodium deoxycholate, 1% SDS, and 0.5% BSA (for GLUT4) or 2% C12E9, 1 μM aprotinin, 1 μM pepstatin, and 1 μM leupeptin (for GLUT1). Collection of immunocomplexes, SDS/PAGE, and immunoblotting were performed as described previously (24), and the proteins were visualized by enhanced chemiluminescence (ECL) or by incubation with ^{125}I-protein A followed by autoradiography. Quantification was performed by densitometric analysis by using OPTILAB image analysis software (Graftek SA, Mirmande, France).

Results

Identification of mUbc9 as a GLUT4-Interactive Protein. To identify GLUT-interactive proteins, a cDNA library derived from TA1 adipocytes was screened with the COOH-terminal domain of rat GLUT4 (residues 467–509) by using a LexA/VP16-based two-hybrid system. The majority of the cDNAs isolated with this method encoded five independent inserts derived from a single gene and fused to VP16 in the same reading frame at different positions in the 5′ untranslated region. Sequence analysis of the longest clone revealed a cDNA with a 5′ untranslated region of 48 bp and an ORF of 474 bp, encoding a protein of 158 aa with a calculated M_r of 18,000. Comparison with sequences in GenBank/European Molecular Biology Laboratory databases demonstrated 100% identity to mUbc9 (20, 28), a recently identified mammalian homologue of Ubc9, which first was cloned as a putative member of the E2 ubiquitin-conjugating enzyme family in yeast (29).

Expression of mUbc9 in Insulin-Sensitive Cells. mUbc9 was detected as a 20-kDa protein in extracts from multiple rat tissues, including skeletal muscle, heart, liver, and kidney, and in a number of cultured cell lines by immunoblotting with anti-mUbc9 antibodies (not shown). In 3T3-L1 adipocytes, mUbc9 was found to be most abundant in high- and low-density microsomal membranes, less abundant in nuclei/mitochondria and plasma membranes, and almost absent in the cytosol, thus overlapping with GLUT4 and GLUT1 glucose transporters in its distribution in these insulin-sensitive cells (Fig. 1). Preferential localization of mUbc9 in intracellular membranes also was observed in L6 skeletal muscle myoblasts (Fig. 1) and terminally differentiated myotubes (data not shown).

Regulation of Cellular Levels of GLUT4 and GLUT1 Transporters by mUbc9. To investigate potential mUbc9 regulatory effects on glucose transporters, mUbc9 or a mUbc9 mutant with substitution of Cys^{93}, in the active site of the enzyme, with Ala (mUbc9-Ala^{93}) was overexpressed in L6 skeletal muscle cells. The mUbc9-Ala^{93} mutant was used as a catalytically inactive dominant negative because it is unable to form sentrin conjugates (30). Multiple clones of L6 skeletal muscle myoblasts stably transfected with pCR3.1 plasmids encoding mUbc9 or mUbc9-Ala^{93} were obtained, and three independent clones of each were selected that overexpressed the mUbc9 and mUbc9-Ala^{93} proteins, respectively, by 2.5- to 3-fold in comparison with nontransfected (wild-type) L6 myoblasts (Fig. 2*A*). Multiple control cell lines were isolated after transfecting cells with the pCR3.1 plasmid lacking an insert (Neo), and levels of mUbc9 protein in Neo control lines were not significantly different from those observed in the nontransfected L6 myoblasts (Fig. 2*A*).

In mUbc9-overexpressing myoblasts, the cellular content of the GLUT4 protein was found to undergo a marked, 8-fold

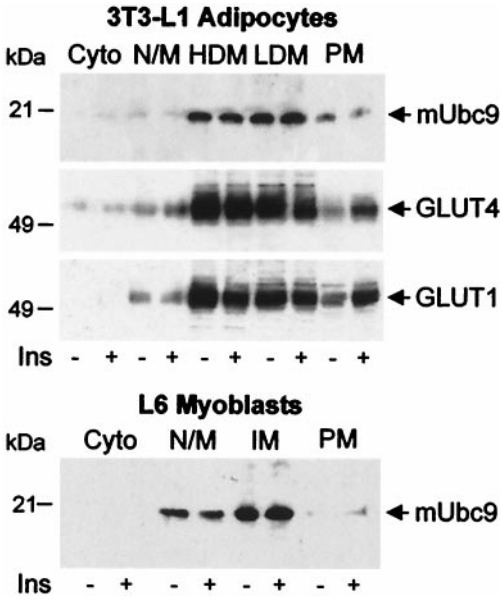

Fig. 1. Predominant localization of mUbc9 protein in intracellular membranes and nuclei/mitochondria of 3T3-L1 adipocytes and L6 myoblasts. Basal or insulin-stimulated (Ins, 1 μM) cells were processed to obtain the cytosol (Cyto), a fraction enriched in nuclei/mitochondria (N/M), high-density microsomes (HDM), low-density microsomes (LDM), and plasma membranes (PM). Intracellular membranes not fractionated into HDM and LDM (IM) were obtained from L6 cells. Equal amounts of protein (10 μg) were subjected to immunoblotting with anti-mUbc9 antibodies. Subcellular fractions from 3T3-L1 adipocytes (10 μg) also were analyzed by immunoblotting with antibodies to GLUT4 or GLUT1, as indicated.

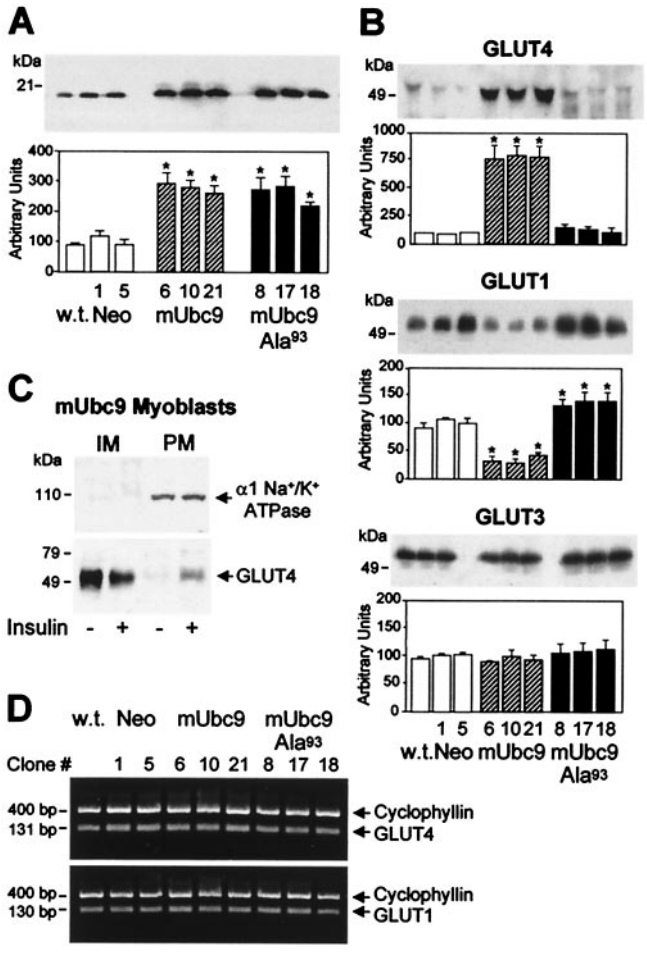

Fig. 2. Regulation of glucose transporters by mUbc9. (*A*) Overexpression of mUbc9 cDNA in L6 myoblasts. L6 cells were left nontransfected (wild type, w.t.) or stably transfected with plasmids encoding mUbc9 (mUbc9, clones 6, 10, and 21), mUbc9 with mutation of Cys^{93} to Ala (mUbc9-Ala^{93}, clones 8, 17, and 18), or the G418 resistance gene alone (Neo, clones 1 and 5). Total cell lysates (10 μg) were analyzed by immunoblotting with anti-mUbc9 antibodies (*Upper*), and the amount of mUbc9 protein was quantified in multiple experiments (*Lower*, mean ± SE of five experiments). *, $P < 0.05$ vs. Neo, clones 1 and 5, and w.t. by unpaired Student's *t* test. (*B*) Effects of mUbc9 or mUbc9-Ala^{93} overexpression on GLUT4, GLUT1, and GLUT3 protein levels in L6 myoblasts. Total cellular membranes (10 μg) from wild-type (w.t.), Neo, mUbc9, or mUbc9-Ala^{93} myoblasts were analyzed by immunoblotting with anti-GLUT4, anti-GLUT1, or anti-GLUT3 antibodies. A representative transporter immunoblot and the quantification of multiple immunoblots (mean ± SE of three experiments) are shown for each. *, $P < 0.05$ vs. Neo, clones 1 and 5, and wild type by unpaired Student's *t* tests. (*C*) GLUT4 transporters in L6 myoblasts overexpressing mUbc9 exhibit insulin-regulatable translocation to the cell surface. IM (10 μg) and PM (10 μg) from basal or insulin-stimulated (1 μM) cells (clone 10) were analyzed by immunoblotting with antibodies to the α1-subunit of Na^+/K^+ ATPase, as a plasma membrane marker (*Upper*), or GLUT4 (*Lower*). IM and PM were depleted or enriched, respectively, in α1 Na^+/K^+ ATPase. GLUT4 levels in IM and PM fractions from Neo or mUbc9-Ala^{93} myoblasts were very low (not shown). (*D*) Unaltered GLUT4 and GLUT1 mRNA levels in nontransfected (w.t.), Neo, mUbc9, and mUbc9-Ala^{93} myoblasts. Total RNA (10 ng) was subjected to reverse transcription–PCR analysis for determination of GLUT4, GLUT1, and cyclophyllin (coamplified in each reaction as a control for amplification efficiency) mRNA levels.

increase in comparison with Neo or wild-type controls (Fig. 2*B Top*, $P < 0.05$). The GLUT4 transporters in mUbc9 myoblasts showed insulin-regulated translocation from intracellular membranes to plasma membranes (Fig. 2*C Bottom*). Overexpression of catalytically inactive mUbc9-Ala^{93} did not modify significantly the characteristic low levels of GLUT4 protein in the L6 myoblasts. From these data, it can be concluded that overexpression of mUbc9, but not mutant mUbc9-Ala^{93}, leads to an increased abundance of functional GLUT4 transporters in L6 cells.

In contrast to the effects of mUbc9 on GLUT4, the total cellular content of the GLUT1 transporter protein was reduced by 65% in myoblasts overexpressing mUbc9 and increased by 35% after transfection with the mUbc9-Ala^{93} mutant in comparison with Neo or wild-type control cells (Fig. 2*B Middle*, $P < 0.05$). The opposite effects of mUbc9 on the GLUT4 and GLUT1 proteins were specific for these transporters, as evidenced by unaltered levels of GLUT3, an additional transporter isoform present in L6 myoblasts, after overexpression of either mUbc9 or mUbc9-Ala^{93} (Fig. 2*B Bottom*). As shown in Fig. 2*D*, GLUT4 and GLUT1 mRNA levels were not different in mUbc9, mUbc9-Ala^{93}, and control myoblasts (GLUT4/cyclophyllin mRNA ratio was 0.571 ± 0.006, 0.572 ± 0.007, 0.568 ± 0.002, and 0.567 ± 0.010, and GLUT1/cyclophyllin mRNA ratio was 0.569 ± 0.021, 0.572 ± 0.007, 0.570 ± 0.001, and 0.561 ± 0.007 in wild-type, Neo, mUbc9, and mUbc9-Ala^{93} myoblasts, respectively, not statistically significant). Thus, the changes in the amounts of the two transporter proteins in these cells do not result from altered expression of the GLUT4 and GLUT1 genes, but likely reflect distinct posttranscriptional effects on the two transporter isoforms.

Modulation of Glucose Transport by mUbc9. The opposite regulation of GLUT4 and GLUT1 by mUbc9 results in significant changes in glucose transport. Overexpression of mUbc9 resulted in markedly reduced basal transport in each of the individual mUbc9 clones, with a mean 60% decrease in comparison with wild-type or Neo myoblasts (Fig. 3, $P < 0.05$). The fold stimulation of glucose transport by insulin was enhanced significantly

CELL BIOLOGY

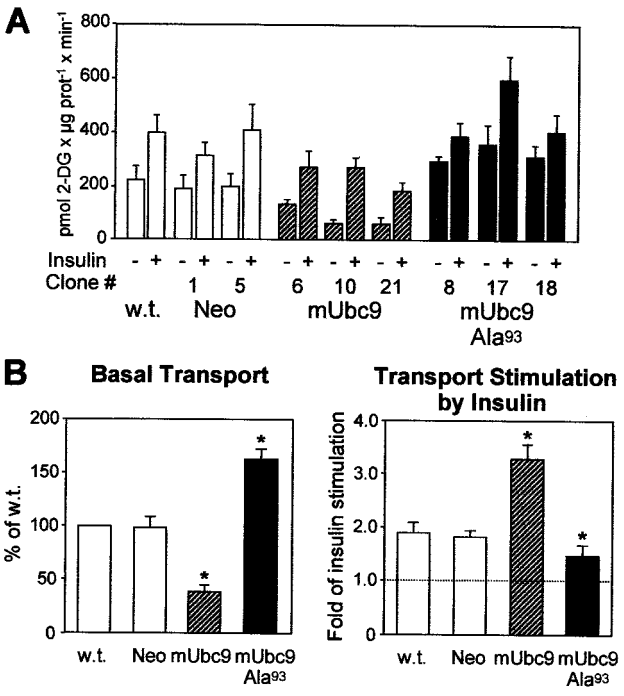

Fig. 3. Modulation of glucose transport by mUbc9. (*A*) Basal and insulin-stimulated glucose transport rates in wild-type (w.t.), Neo, mUbc9, and mUbc9-Ala^{93} myoblasts. Cells cultured in 35-mm diameter wells were serum-starved overnight and then incubated in the presence or absence of 1 μM insulin for 30 min. Transport was started by adding 1 μCi/ml 2-[^{3}H]deoxy-D-glucose (NEN) to a concentration of 50 μM for 10 min at 20°C. (*B*) Basal glucose transport (*Left*) and the fold stimulation of glucose transport by insulin (*Right*) in nontransfected (w.t.), Neo, mUbc9, and mUbc9-Ala^{93} L6 myoblasts. The results represent mean values of four independent experiments performed on individual L6 clones. *, $P < 0.05$ vs. Neo and wild type by unpaired Student's *t* tests.

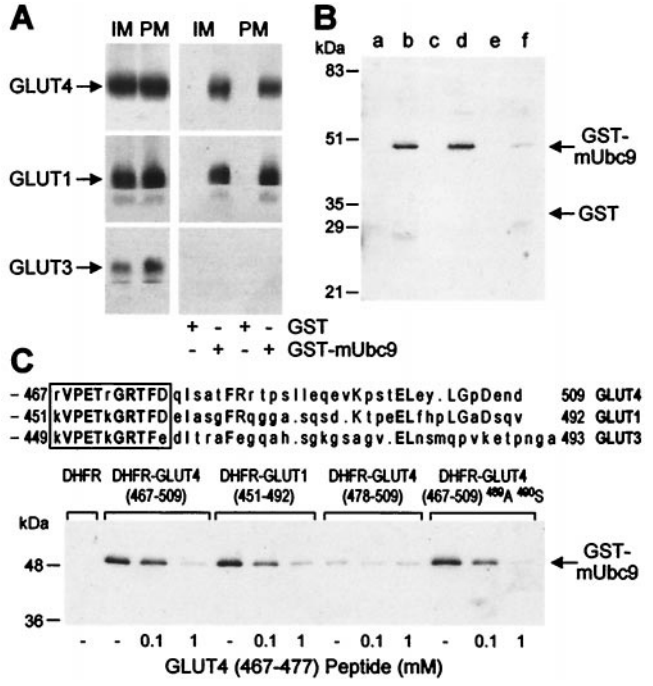

Fig. 4. Association of mUbc9 with glucose transporters. (*A*) Binding of recombinant mUbc9 to GLUT4 and GLUT1, but not GLUT3. GST-mUbc9 or GST (850 nM) was incubated with 75 μg of detergent-solubilized IM and PM from L6 myoblasts overexpressing GLUT4. Transporters bound to the GST fusion proteins were detected by immunoblotting with anti-GLUT4, anti-GLUT1, or anti-GLUT3 antibodies (*Right*). Solubilized membranes (10 μg) were analyzed by immunoblotting to determine their content of GLUT4, GLUT1, and GLUT3 (*Left*). (*B*) Association of GST-mUbc9 with recombinant COOH-terminal fragments of GLUT4 and GLUT1 *in vitro*. COOH-terminal fragments of GLUT4 or GLUT1 fused to hexahistidine-tagged DHFR (6xHis-DHFR, 850 nM) were incubated with GST-mUbc9 or GST (250 nM). The GST fusion proteins associated with the 6xHis-DHFR fusions were detected by immunoblotting with anti-GST antibodies. Lanes: a, 6xHis-DHFR plus GST; b, 6xHis-DHFR-GLUT1 (residues 451–492) plus GST-mUbc9; c, 6xHis-DHFR-GLUT1 (residues 451–492) plus GST; d, 6xHis-DHFR-GLUT4 (residues 467–509) plus GST-mUbc9; e, 6xHis-DHFR-GLUT4 (residues 467–509) plus GST; f, 6xHis-DHFR plus GST-mUbc9. (*C*) Transporter domain responsible for mUbc9 binding. (*Upper*) COOH-terminal sequences of rat GLUT4, rat GLUT1, and rat GLUT3 after the 12th putative transmembrane domain. Amino acid identities in GLUT4 and GLUT1 (uppercase letters) and in GLUT4, GLUT1, and GLUT3 (bold, uppercase letters) are indicated. The boxed amino acid sequences represent highly homologous regions in the transporters. (*Lower*) Effects of a peptide corresponding to residues 467–477 of rat GLUT4 on the association between GST-mUbc9 and various COOH-terminal fragments of GLUT4 or GLUT1. DHFR-GLUT4 (467–509) ^{489}A ^{490}S indicates a variant of the GLUT4 COOH terminus (residues 467–509) with substitution of Leu^{489} and Leu^{490} by Ala and Ser, respectively.

in mUbc9 myoblasts, with a mean 3.3-fold transport increase as compared with 1.8-fold in wild-type and Neo controls (Fig. 3, $P < 0.05$). By contrast, overexpression of the catalytically inactive mUbc9-Ala^{93} protein resulted in increased basal transport (65% increase, $P < 0.05$, Fig. 3) and a 43% reduction of the fold stimulation of glucose uptake by insulin ($P < 0.05$, Fig. 3).

Interaction of mUbc9 with GLUT4 and GLUT1 Involves an 11-aa Sequence in the Transporter COOH Terminus. The basis for the interaction between mUbc9 and glucose transporters was studied further *in vitro*. To test whether purified mUbc9 could bind directly to glucose transporters expressed in mammalian cells, a full-length recombinant mUbc9 protein fused to GST was immobilized on glutathione-Sepharose beads and incubated with solubilized intracellular or plasma membranes of L6 myoblasts overexpressing GLUT4. As shown in Fig. 4*A*, the GST-mUbc9 fusion bound to GLUT4 and GLUT1 transporters. By contrast, no association was observed between the transporters and GST alone or between mUbc9 and GLUT3 transporters.

To map the transporter domain that binds to mUbc9, the direct association of mUbc9 with recombinant COOH-terminal fragments of GLUT4 and GLUT1 produced as fusions with DHFR was evaluated. GST-mUbc9 bound to DHFR fusions containing the COOH-terminal domains of GLUT4 and GLUT1, but not to DHFR alone, and no association was observed between GST and any of the DHFR fusions (Fig. 4*B*). The ability of mUbc9 to associate with both GLUT4 and GLUT1 at the COOH terminus suggested that mUbc9 binds to a homologous amino acid region in the two transporters. Because residues 467–477 of rat GLUT4 and residues 451–461 of rat GLUT1 are 82% identical (Fig. 4*C*), representing a candidate binding site for mUbc9, the association of mUbc9 with a shortened GLUT4 COOH-terminal fragment lacking residues 467–477 was evaluated and found to be greatly reduced (Fig. 4*C*). By contrast, mutation of Leu^{489} and Leu^{490}, distal to amino acids 467–477 of rat GLUT4, did not affect the interaction with mUbc9 (Fig. 4*C*). Furthermore, a synthetic peptide corresponding to residues 467–477 of rat GLUT4 inhibited the association of mUbc9 with the GLUT4 and GLUT1 COOH-terminal fusion proteins, including the GLUT4 fragment with mutation of Leu^{489} and Leu^{490}, in a dose-dependent manner (Fig. 4*C*). A peptide of the same composition with a scrambled sequence (Pro-Arg-Arg-Thr-Glu-Arg-Asp-Phe-Val-Thr-Gly) had no effect on these associations (not shown). Thus, mUbc9 interacts with GLUT4 (and probably GLUT1) by binding to a previously

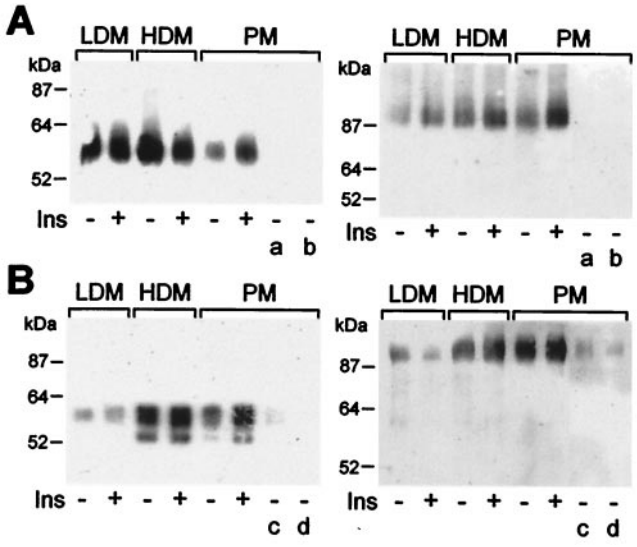

Fig. 5. Covalent modification of GLUT4 and GLUT1 by sentrin conjugation. Solubilized membrane fractions from basal or insulin-stimulated (100 nM) 3T3-L1 adipocytes were subjected to immunoprecipitation with monoclonal anti-GLUT4 (*A*) or polyclonal anti-GLUT1 (*B*) antibodies. Negative control immunoprecipitations were performed with unrelated antibodies (a, monoclonal antiphosphotyrosine; b, monoclonal antiinsulin receptor; c, polyclonal antiphosphotyrosine; d, polyclonal anti-IRS-1). Immunoprecipitates then were subjected to immunoblotting with polyclonal anti-GLUT4 (*A Left*), polyclonal anti-sentrin-1 (*A Right*), polyclonal anti-GLUT1 (*B Left*), or monoclonal anti-sentrin-1 (*B Right*) antibodies.

unrecognized functional domain involving the initial 11 aa of the transporter COOH terminus.

Covalent Modification of GLUT4 and GLUT1 by Conjugation with the mUbc9 Substrate, Sentrin. Sentrin, the specific substrate for the conjugating activity of mUbc9 (31, 32), recently has been renamed sentrin-1, after the identification of two additional polypeptides sharing higher homology with sentrin than with ubiquitin (33). To test whether GLUT4 and GLUT1 are covalently modified by attachment of sentrin-1, solubilized membrane fractions from basal and insulin-treated 3T3-L1 adipocytes were subjected to immunoprecipitation with anti-GLUT4 or anti-GLUT1 antibodies, and the immunoprecipitates were analyzed by immunoblotting with antibodies to sentrin-1. A 90-kDa protein was detected by anti-sentrin-1 antibodies in both anti-GLUT4 and anti-GLUT1 immunoprecipitates, but not in immunoprecipitates obtained with unrelated antibodies (Fig. 5). The 90-kDa protein was found in low-density microsome, high-density microsome, and plasma membrane fractions from basal and insulin-treated cells (Fig. 5). Because sentrin-1 has a molecular mass of 18 kDa, this 90-kDa protein is consistent with the addition of two sentrin-1 molecules to glucose transporters. To demonstrate the sentrin-conjugated transporters in Fig. 5, 9-fold greater amounts of the glucose transporter immunoprecipitates were immunoblotted with anti-sentrin-1 as compared with antiglucose transporter antibodies. Because anti-GLUT4, anti-GLUT1, and anti-sentrin-1 antibodies exhibited similar blotting efficiencies for their respective fusion proteins (data not shown), the immunoprecipitation data suggest that a relatively small percentage of glucose transporters are conjugated to sentrin in 3T3-L1 adipocytes.

Discussion

The sentrin-conjugating enzyme mUbc9 is identified in this study as a GLUT4 and GLUT1 interactive protein that modulates transporter levels in insulin-sensitive cells. Augmented mUbc9 expression in L6 myoblasts results in a decrease in the cellular content of GLUT1 and increase in GLUT4, and these changes correlate with lower basal glucose transport and higher fold stimulation of glucose transport by insulin. The increase in total GLUT4 after mUbc9 overexpression resulted in a greater abundance of transporters capable of translocating from an intracellular site to the plasma membrane in response to insulin (Fig. 2*C*), indicating that GLUT4 was properly sorted to the insulin-responsive compartment and that insulin-signaling mechanisms were preserved in mUbc9 myoblasts. By contrast, introducing the catalytically inactive mUbc9 mutant, mUbc9-Ala^{93}, leads to low GLUT4 and increased GLUT1 levels and concordant increased basal glucose uptake and decreased insulin stimulation of glucose uptake. This likely results from dominant-negative inhibition of endogenous mUbc9 by the mutant enzyme, indicating that mUbc9 regulation of the glucose transport system requires the catalytic activity of the enzyme and also suggesting that changes of GLUT4 and GLUT1 may occur through mUbc9-mediated transporter sentrinization. These observations are in agreement with previous work in other experimental systems, showing that the ability to form thioester conjugates is essential for mUbc9 function (30).

In mUbc9-overexpressing myoblasts, the fold insulin stimulation of glucose transport was increased, but absolute insulin-stimulated glucose transport rates were not different or slightly decreased (Fig. 3*A*), even though GLUT4 content was increased severalfold (Fig. 2*B*). In interpreting these results, it should be considered that mUbc9 effects on glucose transport reflect absolute changes in glucose transporter levels in the context of the relative abundance of individual transporter isoforms in L6 myoblasts. Unlike normal muscle tissue, L6 myoblasts express greater amounts of GLUT1 and GLUT3 than GLUT4, and the stimulation of glucose transport by insulin in L6 cells involves significant insulin-regulated translocation of GLUT1 to the cell surface (26). Thus, reduced GLUT1 levels in L6 myoblasts would be expected to result in a coordinate decrease of basal as well as insulin-stimulated glucose transport rates. In mUbc9-overexpressing compared with control myoblasts, insulin-stimulated transport was decreased by 38%, whereas basal transport was more markedly reduced by 60% (Fig. 3). This difference may be explained by counteracting effects of up-regulation of GLUT4 and down-regulation of GLUT1. Previous studies have shown that GLUT4 must be overexpressed more than 15-fold to produce major effects on insulin-stimulated transport rates in L6 myoblasts (34). It is possible that mUbc9-mediated up-regulation of GLUT4 would lead to more substantial increases in insulin-stimulated glucose transport in cells in which GLUT4 is the predominant transporter isoform.

Although both GLUT4 and GLUT1 interact with mUbc9 and are sentrin-conjugated, the two transporters are regulated by mUbc9 in an opposite manner. Modulation of the amount of GLUT4 and GLUT1 proteins by mUbc9 is not explained by changes in transporter mRNA levels (Fig. 2*D*), suggesting that mUbc9 regulates transporter protein turnover. In a recent study, mUbc9 was shown to modulate degradation of IκBα, a cytosolic protein that binds to NF-κB and prevents the nuclear localization and transcriptional activity of NF-κB (30). In a similar manner, mUbc9 may direct GLUT1 transporters to proteasome- or lysosome-mediated degradation and, thus, explain the reduced total cellular levels of GLUT1 observed in mUbc9-overexpressing myoblasts. mUbc9 was demonstrated recently to direct RanGAP1 to the nuclear pore complex (17–19) and to regulate the partitioning of the promyelocytic leukemia (PML) gene product between the soluble nucleoplasmic fraction and the nuclear bodies (35), consistent with a role for this enzyme in protein-targeting mechanisms. In contrast to GLUT1, the GLUT4 transporter shows an intrinsic tendency to be seques-

tered in a specific storage compartment (4–6), and this correlates with the observed longer half-life of GLUT4 in insulin-sensitive cells (36). We speculate that mUbc9 may mobilize GLUT4 from the Golgi complex or other subcellular compartments and promote targeting to the GLUT4 storage compartment. This could result in a slower GLUT4 turnover and increased cellular abundance of GLUT4, as observed after mUbc9 overexpression.

In studying the region of interaction of mUbc9 with glucose transporters, we have shown that mUbc9 binding occurs through a specific membrane-proximal domain in the GLUT4 and GLUT1 transporters. This region is distinct from the dileucine motif at Leu^{489}-Leu^{490}, which mediates the intracellular sequestration of GLUT4 and is absent in GLUT1 (9, 10). A GLUT4 construct mutated in the dileucine motif was found to bind mUbc9 normally (Fig. 4*C*), suggesting further that the mechanism implicated in transporter regulation by mUbc9 and the trafficking event mediated by the dileucine motif are different. No association of mUbc9 with GLUT3 was detected (Fig. 4*A*), even though GLUT3 contains a sequence that is very similar to the identified mUbc9-binding region in GLUT4 and GLUT1 (Fig. 4*C*). The basis for the absence of mUbc9 binding to GLUT3 has not been defined yet, but it is possible that other amino acid sequences in the GLUT3 COOH terminus inhibit mUbc9 binding to the transporter. In the COOH-terminal domain, GLUT4 and GLUT1 exhibit greater sequence homology with each other than with GLUT3 (Fig. 4*C*). The more divergent sequence of GLUT3 may result in structural features that inhibit or fail to promote mUbc9 binding and its consequent regulatory activities.

Opposite changes in GLUT4 and GLUT1 abundance occur during differentiation of skeletal muscle and fat cells (37, 38) and in skeletal muscle as a consequence of diabetes (39). Expression of the GLUT4 gene is reduced, whereas GLUT4 protein half-life is prolonged in adipocytes from diabetic rats, indicating independent regulation of glucose transporter content at transcriptional and posttranslational levels in this disease (40). Further characterization of factors regulating mUbc9 expression and/or activity should give insight into the mechanism and importance of glucose transport modulation by mUbc9 in normal and pathological states.

We thank G. D. Holman for anti-GLUT1 antibodies, F. Melchior for anti-sentrin-1 antibodies, and K. J. Sweadner for antibody to the α1-subunit of Na^+/K^+ ATPase. This work was supported in part by grants from the Juvenile Diabetes Foundation International, the European Commission (BIOMED2 Program, contract no. BMH4-CT98–3084), and the Ministero dell'Università e Ricerca Scientifica e Tecnologica (Italy) to F.G., and the American Diabetes Association, the Boehringer Mannheim Corporation, the Adler Foundation, and the National Institutes of Health (Diabetes and Endocrinology Research Center Grant DK36836) to R.J.S.

1. Bell, G. I., Burant, C. F., Takeda, J. & Gould, G. W. (1993) *J. Biol. Chem.* **268,** 19161–19164.
2. Pessin, J. E. & Bell, G. I. (1992) *Annu. Rev. Physiol.* **54,** 911–930.
3. Piper, R. C., Hess, L. J. & James, D. E. (1991) *Am. J. Physiol.* **260,** C570–C580.
4. Slot, J. W., Geuze, H. J., Gigengack, S., Lienhard, G. E. & James, D. E. (1991) *Proc. Natl. Acad. Sci. USA* **88,** 7815–7819.
5. Rodnick, K. J., Slot, J. W., Studelska, D. R., Hanpeter, D. E., Robinson, L. J., Geuze, H. J. & James, D. E. (1992) *J. Biol. Chem.* **267,** 6278–6285.
6. Haney, P. M., Slot, J. W., Piper, R. C., James, D. E. & Mueckler, M. (1991) *J. Cell Biol.* **114,** 689–699.
7. Hudson, A. W., Ruiz, M. L. & Birnbaum, M. J. (1992) *J. Cell Biol.* **116,** 785–797.
8. Piper, R. C., Tai, C., Kulesza, P., Pang, S., Warnock, D., Baenziger, J., Slot, J. W., Geuze, H. J., Puri, C. & James, D. E. (1993) *J. Cell Biol.* **121,** 1221–1232.
9. Corvera, S., Chawla, A., Chakrabarti, R., Joly, M., Buxton, J. & Czech, M. P. (1994) *J. Cell Biol.* **126,** 979–989.
10. Vehrey, K. J. & Birnbaum, M. J. (1994) *J. Biol. Chem.* **269,** 2353–2356.
11. Verhey, K. J., Yeh, J.-I. & Birnbaum, M. J. (1995) *J. Cell Biol.* **130,** 1071–1079.
12. Haney, P. M., Levy, M. A., Strube, M. S. & Mueckler, M. (1995) *J. Cell Biol.* **129,** 641–658.
13. Jung, C. Y. (1998) *Exp. Physiol.* **83,** 267–273.
14. Kao, A. W., Noda, Y., Johnson, J. H., Pessin, J. E. & Saltiel A. R. (1999) *J. Biol. Chem.* **274,** 17742–17747.
15. Boddy, M. N., Howe, K., Etkin, L. D., Solomon, E. & Freemont, P. S. (1996) *Oncogene* **13,** 971–982.
16. Kamitani, T., Nguyen, H. P. & Yeh, E. T. H. (1997) *J. Biol. Chem.* **272,** 14001–14004.
17. Mahajan, R., Delphin, C., Guan, T., Gerace, L. & Melchior, F. (1997) *Cell* **88,** 97–107.
18. Matunis, M. J., Coutavas, E. & Blobel, G. (1996) *J. Cell Biol.* **135,** 1457–1470.
19. Matunis, M. J., Wu, J. & Blobel, G. (1998) *J. Cell Biol.* **140,** 499–509.
20. Hateboer, G., Hijmans, E. M., Nooij, J. B. D., Schlenker, S., Jentsch, S. & Bernards, R. (1996) *J. Biol. Chem.* **271,** 25906–25911.
21. Schwarz, S. E., Matuschewski, K., Liakopoulos, D., Scheffner, M. & Jentsch, S. (1998) *Proc. Natl. Acad. Sci. USA* **95,** 560–564.
22. Hollenberg, S. M., Sternglanz, R., Cheng, P. F. & Weintraub, H. (1995) *Mol. Cell. Biol.* **15,** 3813–3822.
23. Schiestl, R. H. & Gietz, R. D. (1989) *Curr. Genet.* **16,** 339–346.
24. Giorgino, F., Pedrini, M. T., Matera, L. & Smith, R. J. (1997) *J. Biol. Chem.* **272,** 7455–7463.
25. Robinson, L. J. & James, D. E. (1992) *Am. J. Physiol.* **263,** E383–E393.
26. Bilan, P. J., Mitsumoto, Y., Ramlal, T. & Klip, A. (1992) *FEBS Lett.* **298,** 285–290.
27. Lu, T., Van Dyke, M. & Sawadogo, M. (1993) *Anal. Biochem.* **213,** 318–322.
28. Wright, D. A., Futcher, B., Ghosh, P. & Geha, R. S. (1996) *J. Biol. Chem.* **271,** 31037–31043.
29. Seufert, W., Futcher, B. & Jentsch, S. (1995) *Nature (London)* **373,** 78–81.
30. Tashiro, K., Pando, M. P., Kanegae, Y., Wamsley, P. M., Inoue, S. & Verma, I. M. (1997) *Proc. Natl. Acad. Sci. USA* **94,** 7862–7867.
31. Desterro, J. M., Rodriguez, M. S. & Hay, R. T. (1998) *Mol. Cell* **2,** 233–239.
32. Gong, L., Kamitani, T., Fujise, K., Caskey, L. S. & Yeh, E. T. H. (1997) *J. Biol. Chem.* **272,** 28198–28201.
33. Kamitani, T., Kito, K., Nguyen, H. P., Fukuda-Kamitani, T. & Yeh, E. T. H. (1998) *J. Biol. Chem.* **273,** 11349–11353.
34. Robinson, R., Robinson, L. J., James, D. E. & Lawrence, J. C., Jr. (1993) *J. Biol. Chem.* **268,** 22119–22126.
35. Müller, S., Matunis, M. J. & Dejean, A. (1998) *EMBO J.* **17,** 61–70.
36. Sargeant, R. J. & Paquet, M. R. (1993) *Biochem. J.* **290,** 913–919.
37. Mitsumoto, Y. & Klip, A. (1992) *J. Biol. Chem.* **267,** 4957–4962.
38. Santalucia, T., Camps, M., Castello, A., Munoz, P., Nuel, A., Testar, X., Palacin, M. & Zorzano, A. (1992) *Endocrinology* **130,** 837–846.
39. Napoli, R., Davalli, A. M., Hirshman, M. F., Weitgasser, R., Weir, G. C. & Horton, E. S. (1996) *J. Clin. Invest.* **97,** 1389–1397.
40. Kim, S.-S., Bae, J. W. & Jung, C. Y. (1994) *Am. J. Physiol.* **267,** E132–E139.